Multivalent immune complexes divert FcRn to lysosomes by exclusion from recycling sorting tubules

Andrew W. Weflen[a,b], Nina Baier[a], Qing-Juan Tang[a,c], Malon Van den Hof[a,d], Richard S. Blumberg[b,e,f], Wayne I. Lencer[a,b,e], and Ramiro H. Massol[a,b,e]

[a]Division of Gastroenterology, Boston Children's Hospital, [b]Department of Pediatrics, Harvard Medical School, [e]Harvard Digestive Diseases Center, and [f]Division of Gastroenterology, Brigham and Women's Hospital, Boston, MA 02115; [d]Department of Biomedical Science, University of Amsterdam, 1012 WX Amsterdam, Netherlands; [c]College of Food Science and Engineering, Ocean University of China, Qingdao 266003, China

ABSTRACT **The neonatal receptor for immunoglobulin G (IgG; FcRn) prevents IgG degradation by efficiently sorting IgG into recycling endosomes and away from lysosomes. When bound to IgG-opsonized antigen complexes, however, FcRn traffics cargo into lysosomes, where antigen processing can occur. Here we address the mechanism of sorting when FcRn is bound to multivalent IgG-opsonized antigens. We find that only the unbound receptor or FcRn bound to monomeric IgG is sorted into recycling tubules emerging from early endosomes. Cross-linked FcRn is never visualized in tubules containing the unbound receptor. Similar results are found for transferrin receptor, suggesting a general mechanism of action. Deletion or replacement of the FcRn cytoplasmic tail does not prevent diversion of trafficking to lysosomes upon cross-linking. Thus physical properties of the lumenal ligand–receptor complex appear to act as key determinants for sorting between the recycling and lysosomal pathways by regulating FcRn entry into recycling tubules.**

Monitoring Editor
Jean E. Gruenberg
University of Geneva

Received: Apr 1, 2013
Revised: May 8, 2013
Accepted: May 28, 2013

INTRODUCTION

It has long been known that cell surface receptors involved in nutrient uptake, signal transduction, and phagocytosis are diverted from recycling to degradative pathways upon receptor cross-linking (Mellman and Plutner, 1984; Mellman *et al.*, 1984; Neutra *et al.*, 1985; Marsh *et al.*, 1986; Ukkonen *et al.*, 1986). How cells sense the oligomerization of membrane proteins to trigger such a switch in intracellular trafficking is unclear. This is particularly relevant for protein receptors that switch between recycling and degradative pathways upon cross-linking with important physiological consequences, as in the case of the immunoglobulin G (IgG) trafficking receptor FcRn.

Internalized cargoes destined for recycling are concentrated in narrow-diameter tubules that emerge from the early sorting endosome, whereas cargoes destined for degradation in lysosomes are excluded from these structures (Geuze *et al.*, 1987, 1988; Mayor *et al.*, 1993; Mukherjee and Maxfield, 2000; Maxfield and McGraw, 2004; Hsu *et al.*, 2012). For soluble cargoes, sorting to the lysosome normally occurs passively after the bulk flow of internalized fluid retained within the larger lumenal volume of maturing endosomes (Dunn and Maxfield, 1992). For membrane proteins, however, many are actively sorted away from the recycling pathway to lysosomes by association with the endosomal sorting complex required for transport on the cytoplasmic side of the endosome limiting membrane (Hurley, 2008; Raiborg and Stenmark, 2009).

Similarly, sorting of some membrane proteins into the recycling pathways occurs by active mechanisms involving interaction with vesicle coat proteins and adaptors that bind regions of the protein's cytoplasmic domain (Dai *et al.*, 2004; Hsu *et al.*, 2012). Sorting of many other membrane components into recycling tubules appears to occur passively by bulk flow, following along with the bulk of

This article was published online ahead of print in MBoC in Press (http://www.molbiolcell.org/cgi/doi/10.1091/mbc.E13-04-0174) on June 5, 2013.

Address correspondence to: Wayne I. Lencer (Wayne.Lencer@childrens.harvard.edu), Ramiro H. Massol (ramiro.massol@childrens.harvard.edu).

The authors report no conflict of interest.

Abbreviations used: BFA, brefeldin A; EGFP, enhanced green fluorescent protein; FcRn, neonatal receptor for immunoglobulin G; HA, hemagglutinin; HA-FcRnΔ303-342, mutant FcRn lacking the tail domain; HMEC-1, human microvascular endothelial cells; IgG, immunoglobulin G; IgG-IHH, mutant IgG that cannot bind FcRn; MDCK, Madin–Darby canine kidney; pIgR, polymeric immunoglobulin receptor; TfR, transferrin receptor.

membrane pulled from early endosomes into the tubules (Maxfield and McGraw, 2004), or by biophysical properties that favor inclusion into recycling tubules (Mukherjee and Maxfield, 2000; Chinnapen *et al.*, 2012). In either case, cross-linking of recycling membrane proteins (or lipids; Chinnapen *et al.*, 2012) overrides normal mechanisms for sorting into the recycling pathway and diverts their trafficking to lysosomes. It is believed that cross-linking drives this switch from recycling to degradative pathways by somehow excluding proteins from entry into the narrow recycling tubules that emerge from early endosomes (Mellman *et al.*, 1983, 1984; Mellman and Plutner, 1984; Marsh *et al.*, 1995), but this hypothesis has not been directly tested.

Here we address this problem by using the rapidly recycling receptor for IgG, FcRn. FcRn resides predominantly within endosomal compartments, where it binds IgG at low pH and sorts the immunoglobulin away from lysosomes into the recycling pathway. This activity in vascular endothelial cells explains the extraordinarily long half-life of IgG in circulation (Akilesh *et al.*, 2007; Montoyo *et al.*, 2009). When FcRn binds to multimeric IgG-opsonized antigens or microbes, however, it switches trafficking from recycling to degradation, and this is important for host defense. In dendritic cells, for example, FcRn carries multivalent IgG-based immune complexes to lysosomes to affect antigen processing, presentation, and adaptive immune responses (Qiao *et al.*, 2008; Baker *et al.*, 2011). In epithelial cells, FcRn sequesters IgG-opsonized viral particles for inactivation within lysosomes (Bai *et al.*, 2011).

By simultaneously visualizing the intracellular trafficking of FcRn carrying monomeric IgG, and IgG-immune complexes in live cells, we show that cross-linking FcRn diverts this receptor to lysosomes by preventing entry into recycling tubules. Mutagenesis studies on FcRn implicate geometrical aspects of the lumenal domain of FcRn–cargo complexes as the decisive sorting factors.

RESULTS

Diversion of FcRn to lysosomes

We used human microvascular endothelial cells (HMEC-1) to study how FcRn is diverted from recycling endosomes to lysosomes upon cross-linking. HMEC-1 cells, which lack detectable endogenous Fc receptor activity, were transfected to stably express human β2M and the FcRn heavy chain tagged with the hemagglutinin (HA) epitope on the N-terminal lumenal domain and enhanced green fluorescent protein (EGFP) on the C-terminal cytoplasmic tail (HA-FcRn-EGFP). Cells expressing HA-FcRn-EGFP (HMEC-1-FcRn cells) showed rapid and pH-dependent endocytosis of IgG but no uptake of a mutant IgG that cannot bind FcRn (IgG-IHH; Spiekermann *et al.*, 2002; data not shown; also see Tzaban *et al.*, 2009). The free receptor or when bound to monomeric IgG localized predominantly to endosomes at steady state, with very low localization in lysosomes.

When HMEC-1-FcRn cells were incubated for 3 h at 37°C with IgG-opsonized ovalbumin (Ova; Figure 1, A–C) or IgG-opsonized fluorescent beads (Figure 1, D–F), however, a sizable fraction of these FcRn-bound cargoes were localized to the lysosomal compartment. There was less FcRn in lysosomes after incubations with the smaller IgG-opsonized ovalbumin complex (~15%) compared with IgG-opsonized beads (~40%), implicating an effect of cargo size and/or degree of receptor cross-linking on FcRn trafficking, an effect suggested before to operate on trafficking of the transferrin receptor (TfR; Marsh *et al.*, 1995). No such signal was obtained in cells exposed to Ova or beads opsonized with the mutant IgG-IHH, which cannot bind FcRn (Spiekermann *et al.*, 2002), showing specificity for FcRn-dependent trafficking. We also found that cross-linking FcRn, using primary rat antibodies against the extracellular HA tag (for 1 h at 37°C) followed by secondary goat anti-Fc antibodies (for 3 h at 37°C), neither of which detectably bind human FcRn via their Fc domains, diverted the majority (65%) of the cross-linked receptor to lysosomes. Similar results were obtained in the epithelial cell lines Madin–Darby canine kidney (MDCK) and BSC-1 expressing FcRn. Thus HMEC-1-FcRn cells model the switch in FcRn trafficking observed in dendritic and epithelial cells when internalizing IgG-opsonized antigen (Qiao *et al.*, 2008) or viral particles (Bai *et al.*, 2011).

Trafficking of monomeric IgG by FcRn transits via early endosomes before recycling or transcytosis. To determine whether cross-linked FcRn first entered early endosomes, we treated cells simultaneously with IgG and FcRn-cross-linking antibodies and assessed overlap with the early endosomal marker EEA-1 at early times after uptake. In all cases, FcRn and its ligands were found largely within early endosomes (Figure 2). More than 90% of antibody–cross-linked FcRn colocalized with monomeric IgG–FcRn complexes and EEA-1 (Figure 2, C and D). Thus all FcRn-bound cargoes and antibody–cross-linked receptor complexes share the same early endosomal compartment.

Cross-linked FcRn complexes fail to enter recycling tubules

Trafficking of IgG from early sorting endosomes through the recycling pathway was proposed to occur at least partially via narrow membrane tubules (Prabhat *et al.*, 2007). When FcRn trafficking was observed in live cells, we found that cross-linked FcRn complexes were excluded from FcRn-positive sorting tubules, but FcRn bound to monomeric IgG was not (Figure 3, A and B). To increase the number of recycling tubules for study, we pretreated cells with brefeldin A (BFA; Lippincott-Schwartz *et al.*, 1991). FcRn labeled with fluorophore-conjugated anti-HA primary antibody alone or monomeric IgG was observed in endosomal sorting tubules (Figure 3, C and D), but larger immune complexes formed by cross-linking anti–HA-FcRn with secondary antibodies were not (Figure 3D). Similar results were obtained by induction of tubule formation using overexpression of Rab11 (Supplemental Figure S4). On using much lower concentrations of the primary antibody (Figure 3D), to allow for IgG binding, we observed some spots present in the recycling tubules. These spots could be vesicles containing cross-linked FcRn trafficking along the same microtubule tracks used by the sorting tubules, or they could be small monomeric or low-level cross-linked FcRn complexes contained within the recycling tubules, an interpretation we favor.

To test whether other cell surface receptors were similarly excluded from sorting tubules upon ligand-induced cross-linking, we evaluated the well-studied and structurally unrelated TfR. TfR also rapidly recycles from endosomes to the cell surface and populates almost identical cellular compartments to those occupied by FcRn (Supplemental Figure S1A). TfR was delivered to lysosomes upon primary and secondary antibody–induced cross-linking with kinetics similar to those of FcRn (Supplemental Figure S1, B–D). When bound to transferrin, the TfR was found within sorting tubules (Figure 4A), but after antibody-induced cross-linking, the TfR was not found in sorting tubules (Figure 4B). After cross-linking, both FcRn and TfR were localized instead in large intracellular vesicles presumed to be early endosomes (Figure 4C). Throughout these studies, we recorded many events in which tubules containing ligand-free FcRn, FcRn bound to monomeric IgG, or transferrin bound to TfR emerged from vesicles that also contained the antibody–cross-linked receptors (Figure 4B; see more examples in Supplemental Figure S2, A–D). Without exception, the cross-linked receptors were excluded from the sorting tubules.

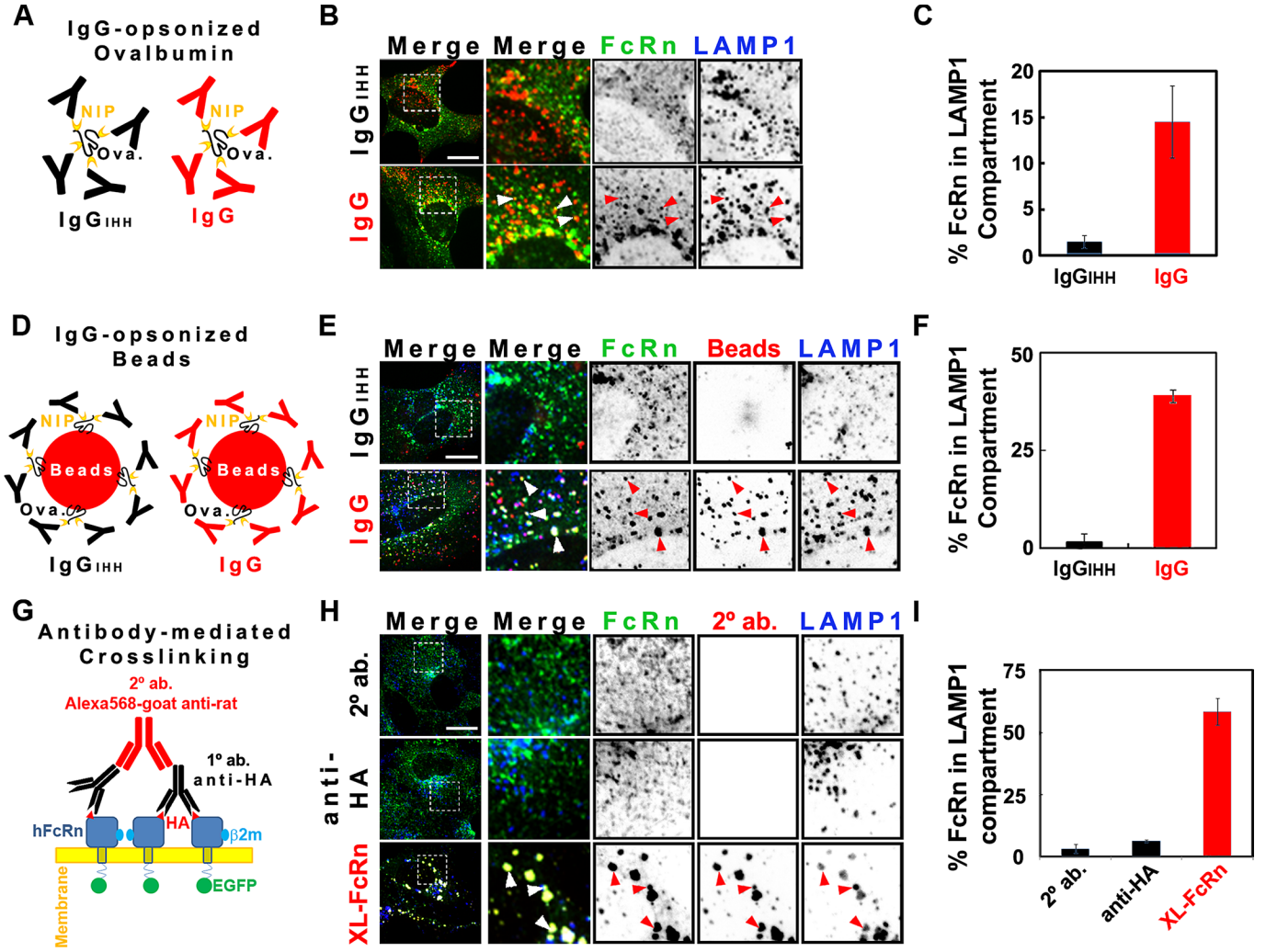

FIGURE 1: Cross-linked HA-FcRn-EGFP is diverted from recycling endosomes to lysosomes. For indirect cross-linking experiments (see models A and D), HMEC-1 cells were incubated at pH 6 with 20 μM NIP-ovalbumin opsonized with IgG (1:5 M ratio; A–C) or 4.5 pM 100-nm IgG-opsonized fluorescent beads (1:100 beads-to-IgG molar ratio; D–F) for 3 h at 37°C. For direct cross-linking experiments (G–I), cells were incubated with HBSS-H buffer (row 1) or primary (rows 2 and 3) rat anti-HA antibodies (2 μg/ml) for 1 h at 37°C in HBSS-H (pH 7.4). Samples were washed with PBS buffer (pH 7.4) and further incubated with HBSS-H (row 2) or secondary (rows 1 and 3) Alexa 568–goat anti-rat antibodies (40 μg/ml) for 3 h at 37°C. Cells were washed, fixed, and stained for LAMP-1 (see *Materials and Methods*). Representative confocal middle sections of each condition are shown, with arrowheads indicating examples of colocalization between HA-FcRn-EGFP, ligands, and LAMP-1. Selected regions (stippled-line squares) were cropped and enlarged and are displayed using an inverted monochrome color scale to aid visualization. Scale bar, 10 μm. Bar plots (C, F, I) depict the quantification calculated by mask analysis (see *Materials and Methods*) of diversion of FcRn to the LAMP-1 compartment (average and SD of three to five independent experiments, $n = 10–20$ cells).

The FcRn transmembrane and cytosolic regions are dispensable for diversion of FcRn to lysosomes

To test whether active sorting is involved in the trafficking of cross-linked FcRn to lysosomes, we studied HMEC-1 cells expressing FcRn lacking the tail domain (HA-FcRnΔ303-342). As in MDCK cells (Claypool *et al.*, 2004; Dickinson *et al.*, 2008), the mutant FcRn localized primarily to the plasma membrane at steady state (Supplemental Figure S3), with small amounts also localized in the EEA-1–positive endosomes (Supplemental Figure S3, A and B). This was unchanged by binding monomeric IgG, but after cross-linking, the mutant receptor was diverted to lysosomes (approximately threefold increase in LAMP-1 colocalization; Supplemental Figure S3, C and D). In live cells, the HA-FcRnΔ303-342 receptor was never visualized in endosomal sorting tubules (data not shown) before or after cross-linking (Figure 5A), implicating active sorting mechanisms for the efficient recycling of FcRn.

We also tested a chimeric receptor comprising the HA-tagged FcRn extracellular domain fused to the transmembrane and cytosolic domains of the polymeric immunoglobulin receptor (pIgR; Figure 5, B and C). pIgR is structurally unrelated to FcRn, but like FcRn, it acts as a trafficking receptor, transporting IgA and IgM across polarized epithelial cells at mucosal surfaces (Kaetzel *et al.*, 1991; Mostov, 1995). The chimeric HA-FcRn-pIgR receptor bound and internalized IgG into early endosomes (data not shown) and was also found in recycling tubules (Supplemental Figure S2E), confirming normal folding and function of the FcRn extracellular and pIgR cytosolic

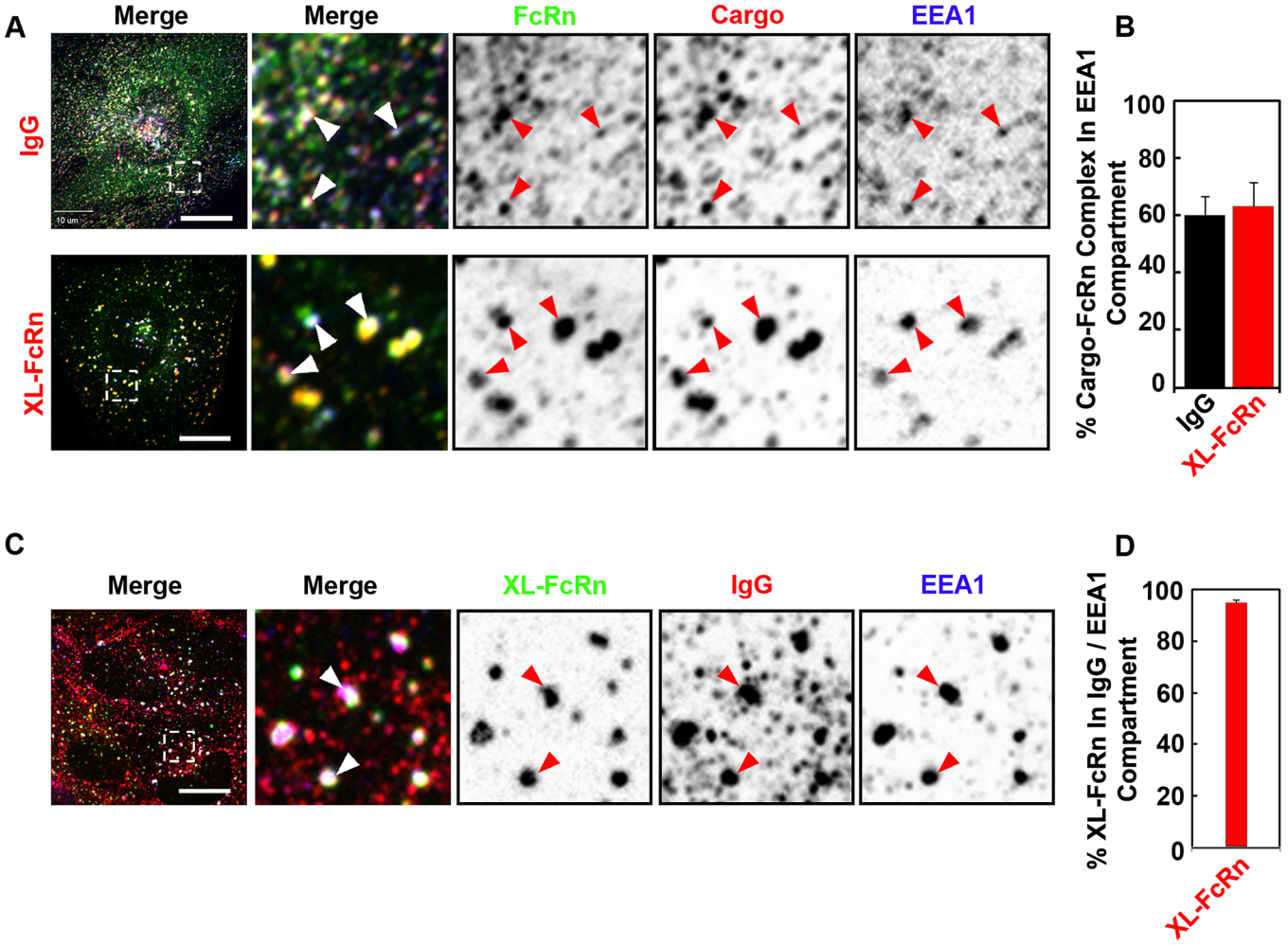

FIGURE 2: Monomeric and cross-linked FcRn complexes are internalized into the same early endosomal compartment. (A, B) IgG or directly cross-linked FcRn is delivered to early endosomes after endocytosis. HMEC-1 cells stably expressing HA-FcRn-EGFP were incubated with either monomeric Alexa 568–human IgG (25 µg/ml) at pH 6 for 15 min at 37°C or with rat anti-HA primary antibodies (2 µg/ml) at pH 7.4 for 30 min at 37°C, followed by Alexa 568–goat anti-rat secondary antibodies (40 µg/ml) for 15 min at 37°C. (C, D) Cross-linked FcRn is internalized into early endosomes containing internalized IgG. HMEC1 cells stably expressing HA-FcRn were first incubated with rat anti-HA primary antibodies (2 µg/ml) at pH 7.4 for 30 min at 37°C, followed by coincubation with monomeric Alexa 568–human IgG (25 µg/ml) and Alexa 488–anti-rat secondary antibodies (40 µg/ml) at pH 6 for 15 min at 37°C. All samples were then fixed and stained for the early endosome antigen 1 (EEA1). Representative confocal middle sections of each condition are shown, with arrowheads indicating examples of colocalization between FcRn, ligands, and EEA1, and displayed as described in the Figure 1 legend. Scale bar, 10 µm. Bar plots show the quantification of fraction of IgG and cross-linked FcRn in the EEA1 compartment (B) or the fraction of cross-linked FcRn in IgG-containing early endosomes (D; average and SD of three independent experiments, $n = 22$ cells).

domains. At steady state the chimeric receptor was enriched at the cell surface, and a small fraction was present in early endosomes (data not shown) and lysosomes (Figure 5, B and C), consistent with the steady-state distribution of pIgR. When cross-linked by primary and secondary antibodies against the extracellular HA tag, the chimeric receptor was sorted to lysosomes (Figure 5, B and C). Thus the transmembrane and cytoplasmic regions of FcRn appear to be dispensable for lysosomal sorting.

DISCUSSION

Our results implicate physical properties of the FcRn lumenal ligand–receptor complex as the decisive factor that blocks entry into recycling tubules and causes the switch in receptor sorting from recycling endosomes to lysosomes, presumably by trapping the cross-linked receptor within the endosomal maturation pathway (Maxfield and McGraw, 2004). It is possible that FcRn is excluded from the narrow lumen of endosome sorting tubules due to the size of the FcRn–cargo complex, as seen for sorting of differentially sized cargoes in macrophages (Berthiaume *et al.*, 1995). Another explanation could be that cross-linking FcRn prevents the receptor from conforming to the high membrane curvatures that typify sorting tubules (Jiang and Powers, 2008) or that cross-linking prevents the assembly of ribbon-like networks caused by IgG linking FcRn heterodimers on closely opposed endosomal membranes (Raghavan and Bjorkman, 1996; Tesar *et al.*, 2006). Our experimental approach cannot discern between effects caused by cargo geometry and cross-linking of FcRn per se. These potential mechanisms are not mutually exclusive, and all could operate in parallel.

Many ideas emerging from earlier work on cross-linking Fc-γ and TfRs presage our experimental results on FcRn (Mellman and

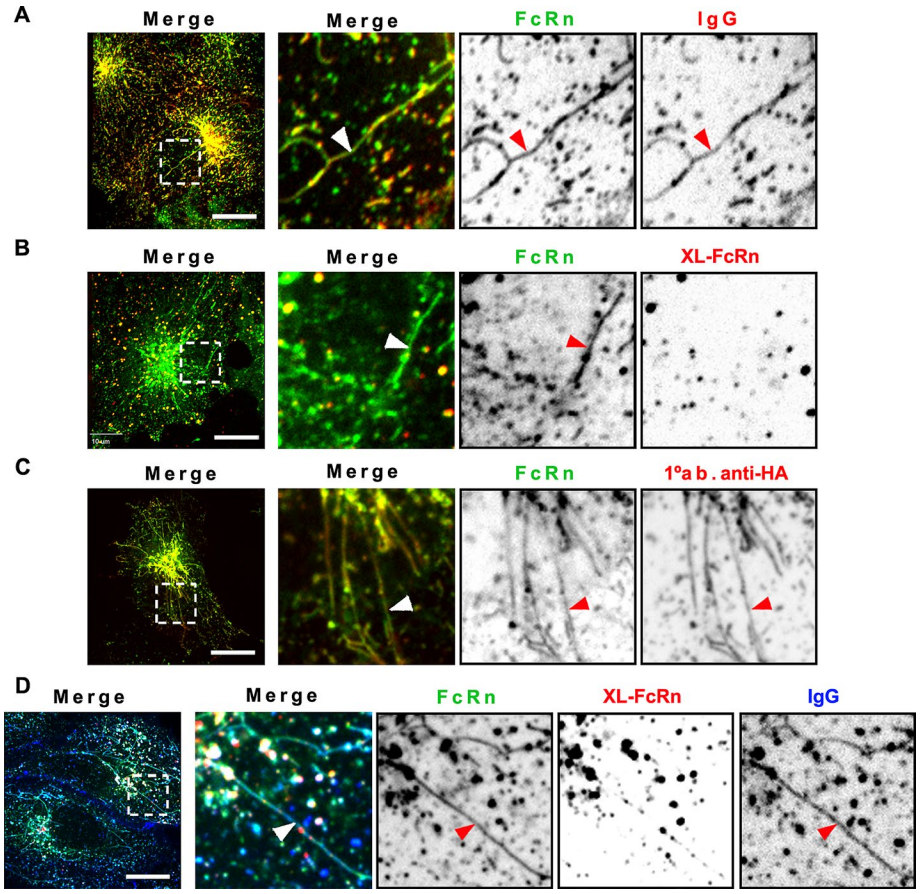

FIGURE 3: Monomeric but not multimeric IgG-FcRn complexes are sorted into recycling tubules. HMEC-1 cells stably expressing HA-FcRn-EGFP were incubated with monomeric Alexa 568–human IgG (25 μg/ml) at pH 6 (A) or Alexa 568–rat anti-HA primary antibody (25 μg/ml) at pH 7.4 for 15 min at 37°C (C). Other samples were incubated with unlabeled rat anti-HA antibody (2 μg/ml, B; 0.2 μg/ml, D) for 1 h at 37°C, followed by further incubation with Alexa 568–goat anti-rat antibody for 15 min at 37°C. Some samples were further incubated with Alexa 647–human IgG (50 μg/ml; D). All samples were then washed and transferred to an open perfusion chamber for live-cell imaging acquisition. To stimulate formation of recycling tubules, some samples (C, D) were incubated with HBSS-H (pH 7.4) containing 10 μM BFA during live-cell imaging acquisition. Time series were recorded with an interval of 2 s. Representative confocal middle sections of each condition are shown, with arrowheads indicating examples of tubules, and displayed as described in the Figure 1 legend. Note the strong increase in sorting tubules, containing IgG, or primary only antibody–FcRn complexes, and large vesicles containing cross-linked FcRn complexes, which are absent from sorting tubules. Scale bars, 10 μm.

Plutner, 1984; Neutra *et al.*, 1985; Marsh *et al.*, 1995), including evidence that lumenal factors dominate the switch to lysosomal pathways after endocytosis (Marsh *et al.*, 1995). None, however, explains how receptors fail to sort into recycling pathways upon cross-linking. Our studies with FcRn, TfR, and the FcRn–pIgR chimera indicate that normally recycling receptors can be excluded from sorting tubules and diverted to lysosomes by multivalent cargo binding and that this is likely a general mechanism of action. Early endosomes also actively sort internalized cargoes retrograde to the *trans*-Golgi network by association with the retromer complex (Bonifacino and Hurley, 2008) and in polarized cells to the opposite membrane surface by transcytosis (He *et al.*, 2008; Tzaban *et al.*, 2009). On the basis of our results, we predict that cross-linking will also block trafficking into these pathways by affecting entry into the narrow-diameter sorting tubules emerging from early endosomes and serving these destinations.

The physiological and evolutionary significance of such a sorting mechanism with respect to FcRn becomes evident in tissues such as lung or gut, where epithelial cells, macrophages, and dendritic cells form a physical and functional barrier against the invasion of pathogens and other environmental antigens. Here cross-linking FcRn by binding IgG-opsonized cargoes and diversion to lysosomes could operate in immune surveillance and host defense. Depending on size and degree of cargo opsonization, it could also act to prevent pathogens from accessing the host by breeching the intestinal or respiratory epithelium after the normal pathway of IgG transport across mucosal surfaces by FcRn-mediated transcytosis. Finally, our results have important implications for the design of therapeutic Fc-fusion proteins with respect to how the size and geometry of these molecules might affect receptor-mediated recycling and thus half-life in circulation.

MATERIALS AND METHODS

Plasmids and molecular cloning

Human FcRn with the murine H2-Kb signal sequence and HA epitope tag fused to the N-terminus and EGFP fused to the C-terminus was expressed from pcDNA3.1/HA-FcRn-EGFP (Tzaban *et al.*, 2009). B2M was expressed from pEF6/V5-His-β2m (Claypool, 2002; Tzaban *et al.*, 2009). The same FcRn construct lacking EGFP was expressed from pLVX-puro (Clontech). Tailless FcRn was created by PCR amplification of the 909 5′ nucleotides of pLVX-HA-FcRn and restriction cloning this fragment into pLVX-puro. DsRed-Rab11 was purchased from Addgene (Cambridge, MA). Rab11-EGFP was a kind gift from T. Kirchhausen (Harvard Medical School, Boston, MA).

The FcRn/pIgR chimera was derived from pIRES-B2M-2A-FcRn-IRES-mThy1.1. This plasmid was created by cloning β2M-2A-FcRn and murine Thy1.1 cDNA into the first and second multiple cloning sites of the pIRES vector (Clontech, Mountain View, CA). B2M was fused to FcRn via a viral 2A peptide, which results in synthesis of a single mRNA that produces two distinct polypeptides via ribosomal skipping at the 2A site during translation (Szymczak *et al.*, 2004). The transmembrane and tail portions of this FcRn construct were replaced with the corresponding regions of human pIgR to produce the FcRn/pIgR chimera. Murine Thy1.1 is a glycosylphosphatidylinositol-anchored protein that localizes to the cell surface and thus serves as an easily detectable proxy for B2M and FcRn expression by virtue of the intervening internal ribosome entry site. Primer sequences and other details regarding plasmid construction are available upon request.

Cell culture and transfection

HMEC-1 cells (a kind gift from Sean Colgan, Division of Gastroenterology, School of Medicine, University of Colorado, Aurora, CO) were maintained in MCDB 131 (Mediatech, Manassas, VA) supplemented with 10% fetal bovine serum (FBS; Invitrogen, Carlsbad, CA), 100 U/ml

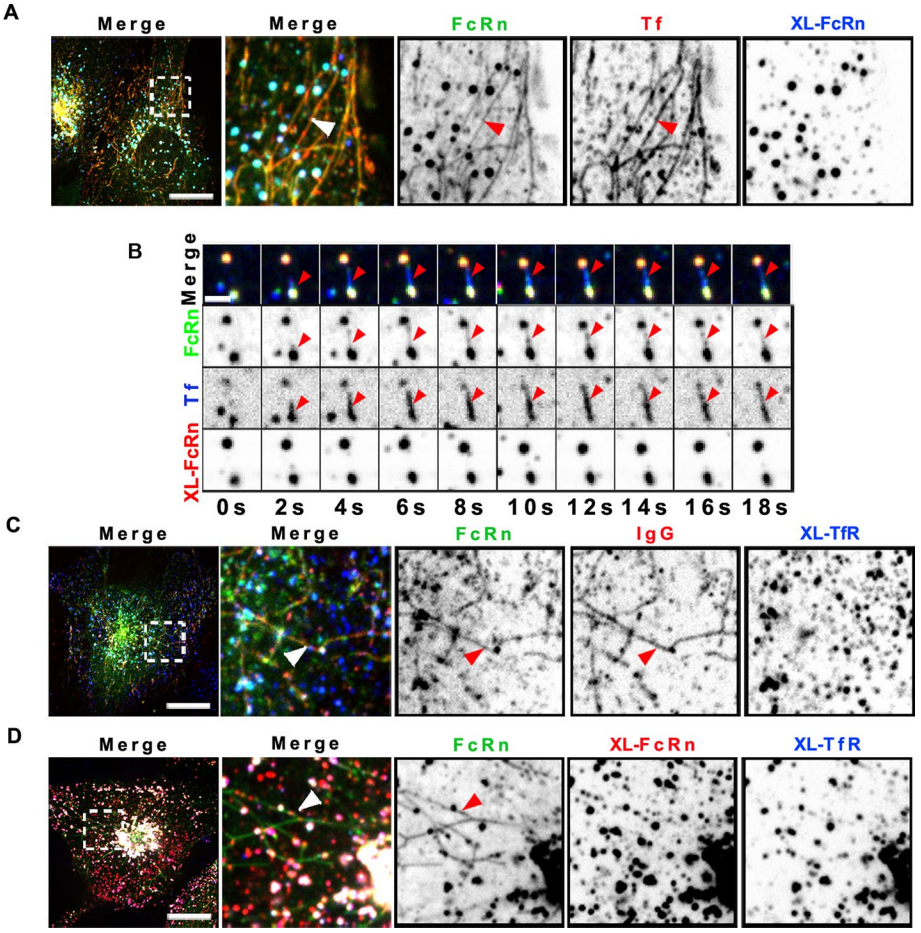

FIGURE 4: Cross-linking TfR also prevents sorting into recycling tubules. HMEC-1 cells stably expressing HA-FcRn-EGFP were incubated with rat anti-HA antibody (2 µg/ml) (A) or mouse anti–TfR ectodomain antibody (25 µg/ml) alone (C) or together with rat anti-HA antibody (D) for 1 h at 37°C. Samples were washed and further incubated with Alexa 568–human transferrin and Alexa 647–goat anti-rat antibody (A), Alexa 647–human transferrin and Alexa 568–goat anti-rat antibody (B), Alexa 568–human IgG and Alexa 647–goat anti-mouse antibody (C), or Alexa 568-goat anti-rat antibodies alone and Alexa 647–goat anti-mouse antibodies (D) for 15 min at 37°C. Samples were then washed and transferred to an open perfusion chamber for live-cell imaging acquisition, and medium containing 10 µM BFA was added. Time series were recorded immediately after the addition of BFA. Representative confocal middle sections of each condition are shown, with arrowheads indicating examples of tubules containing IgG or transferrin and lacking cross-linked TfR and FcRn multimeric complexes, and displayed as described in the Figure 1 legend. Scale bars, 10 µm.

penicillin, 100 µg/ml streptomycin (P/S; Mediatech), and 1 µg/ml hydrocortisone (Sigma-Aldrich, St. Louis, MO). HMEC-1 cells were transfected using either FuGENE 6 (Roche Molecular Biochemicals, Mannheim, Germany) or Xfect (Clontech) following manufacturer's instructions. The following antibiotic concentrations were used to select for stable transgene expression: pcDNA3.1 and pIRES, 1 mg/ml G418 (Mediatech); pEF6/V5-His, 8 µg/ml blasticidin S (EMD, San Diego, CA); and pLVX-Puro, 200 ng/ml Puromycin (EMD). Antibiotic-resistant cells were further screened for transgene expression by fluorescence-activated cell sorting. Cells expressing moderate to high levels of EGFP, where possible, or pH 6–dependent fluorescent IgG binding were collected using a BD FacsAriaII cell sorter (BD Biosciences, San Diego, CA) and maintained in selective media for all experiments.

MDCK II cells stably expressing human HA-FcRn-EGFP (ATCC CRL-2936; Tzaban *et al.*, 2009) were maintained in DMEM supplemented with 2 mM L-glutamine, P/S, and 15% FBS.

Cross-linking and endocytosis experiments

The following were used as model IgG-opsonized particles: 1) purified human IgG (Innovative Research, Novi, MI) conjugated to Qdot 565 Goat F(ab')2 anti-human IgG conjugate (~20 nm; Invitrogen), with excess IgG removed by dialysis against phosphate-buffered saline (PBS) using 50-nm–pore size membranes (Millipore, Billerica, MA); 2) 100-nm-diameter, carboxylate-modified, red fluorescent polystyrene microspheres (FluoSpheres, Invitrogen) adsorbed with NIP-ovalbumin (Biosearch Technologies, Novato, CA) and opsonized with anti-NIP human IgG wild type or IHH. Excess NIP-ova and IgG were removed via repeated centrifugation and resuspension steps using PBS. Recombinant human NIP-specific IgG and NIP-IgG-IHH were purified from supernatants of J558L myeloma cells maintained in RPMI supplemented with 10% FBS, 2 mM L-glutamine, and P/S (Claypool *et al.*, 2004) using protein G and protein A affinity chromatography (GE Healthcare, Piscataway, NJ) and eluted with glycine buffer at pH 3, followed by neutralization. The eluate was dialyzed against PBS and concentrated using Centriprep (Millipore).

Cells were seeded on 18-mm glass coverslips (size 1.5; Warner Instruments, Hamden, CT) 48 h before treatment and then washed with PBS and placed on Parafilm M (VWR, Radnor, PA) inside a humidified chamber. Alexa Fluor–labeled human IgG (Jackson ImmunoResearch Laboratories, West Grove, PA) and IgG-opsonized particles were diluted in Hank's balanced salt solution (HBSS) buffered to pH 6 with 20 mM 2-(*N*-morpholino)ethanesulfonic acid. For direct cross-linking experiments, cells were incubated with 2 µg/ml rat anti-HA antibody (Roche) in HBSS (pH 7.4) for 1 h at 37°C. Unbound anti-HA antibody was removed with PBS. Cells were then further incubated with 40 µg/ml Alexa Fluor 568–labeled goat anti-rat antibodies (Invitrogen) for 2–3 h at 37°C. Where indicated, rat anti-HA antibodies were directly labeled with Alexa 568 using the APEX Antibody Labeling Kit (Invitrogen) following manufacturer's instructions, in which case no secondary incubation was conducted. Antibodies were dialyzed against PBS at room temperature for 30 min using membrane filters with 25-nm pore size (Millipore) to remove sodium azide.

Immunocytochemistry

Cells were washed five times with PBS between steps. All incubations were performed at room temperature. After fixation with 4% paraformaldehyde for 20 min, cells were permeabilized, quenched, and blocked with PBS/50 mM NH_4Cl/5% BSA/0.1 g% saponin for 10 min. Cells were incubated for 1 h with primary antibodies diluted

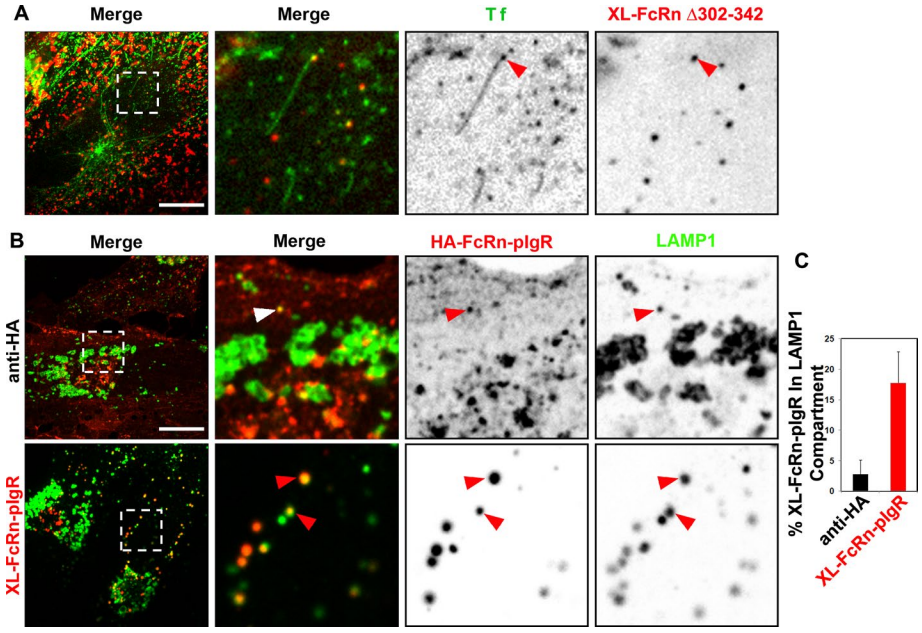

FIGURE 5: Diversion of cross-linked FcRn to lysosomes depends on its lumenal domain. (A) Cross-linked FcRn tailless mutant is not efficiently sorted into recycling tubules. HMEC-1 cells stably expressing HA-FcRnD303-342 were incubated with rat anti-HA antibody (2 μg/ml) for 1 h at 37°C. Samples were then washed and further incubated with Alexa 488–human Tf and Alexa 568–goat anti-rat antibody for 15 min at 37°C. Samples were then washed and transferred to an open perfusion chamber for live-cell imaging acquisition, and medium containing 10 μM BFA was added. Time series were recorded immediately after the addition of BFA. Representative confocal middle sections of each condition are shown, with arrowheads indicating examples of tubules containing transferrin and lacking cross-linked HA-FcRnD303-342 multimeric complexes, and displayed as described in the Figure 1 legend. (B, C) Cross-linked HA-FcRn-pIgR chimeric receptor complexes are delivered into lysosomes. Cells stably expressing HA-FcRn-pIgR were first incubated with rat anti-HA primary antibodies (2 μg/ml) at pH 7.4 for 30 min at 37°C, followed by incubation with Alexa 568–anti-rat secondary antibodies (40 μg/ml) for 30 min at 37°C. All samples were then fixed and stained for LAMP-1. Representative confocal middle sections of each condition are shown, with arrowheads indicating examples of colocalization between FcRn-pIgR and LAMP-1, and displayed as described in the Figure 1 legend. Scale bars, 10 μm. (B) Quantification of fraction of cross-linked FcRn-pIgR in LAMP-1 (average and SD of three independent experiments, $n = 27$ cells).

1:100 in blocking buffer. The early endosomal compartment was labeled with rabbit anti-EEA1 antibodies (Cell Signaling Technology, Beverly, MA). Lysosomes were labeled with mouse monoclonal anti–LAMP-1 antibody (clone H4A3; Developmental Studies Hybridoma Bank, University of Iowa, Iowa City, IA). Cells were then washed and incubated with Alexa Fluor–labeled secondary antibodies (Invitrogen) diluted 1:1000 in blocking buffer, washed, and mounted using Mowiol.

Image acquisition, processing, and analysis

Confocal images were acquired using a spinning disk confocal head (CSU-X1, PerkinElmer, Boston, MA) coupled to a fully motorized inverted Zeiss Axiovert 200M microscope (Carl Zeiss, Jena, Germany) equipped with a 63× lens (Pan Apochromat, 1.4 numerical aperture) and with a 175-W xenon lamp (Lambda DG-4; Sutter Instruments, Novato, CA) for wide-field illumination. Solid-state lasers (473, 568, and 660 nm; Crystal Laser, Reno, NV) were coupled to the spinning head through a fiber optic. An acoustic-optical tunable filter was used to switch between different wavelengths. The imaging system operated under control of SlideBook 5 (Intelligent Imaging Innovations, Denver, CO) and included a computer-controlled spherical aberration correction device (Intelligent Imaging Innovations) installed between the objective lens and the charge-coupled device camera (QuantEM:512SC; Photometrics, Tucson, AZ). Acquisition of sequential optical sections spaced 0.4 μm apart was achieved with the aid of a Piezoelectric Z motorized stage (Applied Scientific Instrumentation, Eugene, OR). For live-cell imaging, cells were placed on 25-mm coverslips (size 1.5; Warner Instruments). Coverslips were transferred into open perfusion chambers (Attofluor, Invitrogen), where they were washed with PBS, and prewarmed medium was added. The chamber was inserted into a sample holder placed on top of the microscope stage enclosed by an environmental chamber (37°C). Most experiments were carried out in HBSS, pH 7.4.

IMAB image analysis and processing software (Massol *et al.*, 2006; Cureton *et al.*, 2009, 2010; Utskarpen *et al.*, 2010) was used to calculate the Manders colocalization coefficients as follows (Manders *et al.*, 1992). Cellular regions containing receptors (FcRn or TfR) and early (EEA-1) or late (LAMP-1) endosomes were masked by segmentation of the corresponding channel with or without uniform background correction by a defined pixel intensity, which typically was greater than twofold the local background. Masks were further refined by eliminating objects <10 voxels in size and occupying fewer than three consecutive *z*-sections. Colocalization masks were obtained by a logical AND operation between the receptor and endosome primary masks. Objects occupying <10 voxels, fewer than three consecutive *z*-sections, or with Pearson's r <0.5 between selected receptor and endosomal channels were removed. Manders coefficients were calculated by dividing the fluorescence intensity under the colocalization mask (overlapping signal) by the fluorescence intensity under the primary mask (total signal). Plots and statistical analysis were performed using Excel 2007 (Microsoft, Redmond, WA).

ACKNOWLEDGMENTS

This study was supported by National Institutes of Health Grants DK084424 (W.I.L., R.H.M.), DK53056 (R.S.B), and 5T32HD7466-14 (A.W.W.), and P30 DK34854 (Harvard Digestive Diseases Center). We thank Marian Neutra for critical reading of the manuscript.

REFERENCES

Akilesh S, Christianson GJ, Roopenian DC, Shaw AS (2007). Neonatal FcR expression in bone marrow-derived cells functions to protect serum IgG from catabolism. J Immunol 179, 4580–4588.

Bai Y, Ye L, Tesar DB, Song H, Zhao D, Bjorkman PJ, Roopenian DC, Zhu X (2011). Intracellular neutralization of viral infection in polarized epithelial cells by neonatal Fc receptor (FcRn)-mediated IgG transport. Proc Natl Acad Sci USA 108, 18406–18411.

Baker K *et al.* (2011). Neonatal Fc receptor for IgG (FcRn) regulates cross-presentation of IgG immune complexes by CD8-CD11b+ dendritic cells. Proc Natl Acad Sci USA 108, 9927–9932.

Berthiaume EP, Medina C, Swanson JA (1995). Molecular size-fractionation during endocytosis in macrophages. J Cell Biol 129, 989–998.
Bonifacino JS, Hurley JH (2008). Retromer. Curr Opin Cell Biol 20, 427–436.
Chinnapen DJ *et al*. (2012). Lipid sorting by ceramide structure from plasma membrane to ER for the cholera toxin receptor ganglioside GM1. Dev Cell 23, 573–586.
Claypool SM (2002). Functional reconstitution of human FcRn in Madin-Darby canine kidney cells requires co-expressed human beta 2-microglobulin. J Biol Chem 277, 28038–28050.
Claypool SM, Dickinson BL, Wagner JS, Johansen FE, Venu N, Borawski JA, Lencer WI, Blumberg RS (2004). Bidirectional transepithelial IgG transport by a strongly polarized basolateral membrane Fcgamma-receptor. Mol Biol Cell 15, 1746–1759.
Cureton DK, Massol RH, Saffarian S, Kirchhausen TL, Whelan SP (2009). Vesicular stomatitis virus enters cells through vesicles incompletely coated with clathrin that depend upon actin for internalization. PLoS Pathog 5, e1000394.
Cureton DK, Massol RH, Whelan SP, Kirchhausen T (2010). The length of vesicular stomatitis virus particles dictates a need for actin assembly during clathrin-dependent endocytosis. PLoS Pathog 6, e1001127.
Dai J, Li J, Bos E, Porcionatto M, Premont RT, Bourgoin S, Peters PJ, Hsu VW (2004). ACAP1 promotes endocytic recycling by recognizing recycling sorting signals. Dev Cell 7, 771–776.
Dickinson BL *et al*. (2008). Ca2+-dependent calmodulin binding to FcRn affects immunoglobulin G transport in the transcytotic pathway. Mol Biol Cell 19, 414–423.
Dunn KW, Maxfield FR (1992). Delivery of ligands from sorting endosomes to late endosomes occurs by maturation of sorting endosomes. J Cell Biol 117, 301–310.
Geuze HJ, Slot JW, Schwartz AL (1987). Membranes of sorting organelles display lateral heterogeneity in receptor distribution. J Cell Biol 104, 1715–1723.
Geuze HJ, Stoorvogel W, Strous GJ, Slot JW, Bleekemolen JE, Mellman I (1988). Sorting of mannose 6-phosphate receptors and lysosomal membrane proteins in endocytic vesicles. J Cell Biol 107, 2491–2501.
He W, Ladinsky MS, Huey-Tubman KE, Jensen GJ, McIntosh JR, Bjorkman PJ (2008). FcRn-mediated antibody transport across epithelial cells revealed by electron tomography. Nature 455, 542–546.
Hsu VW, Bai M, Li J (2012). Getting active: protein sorting in endocytic recycling. Nat Rev Mol Cell Biol 13, 323–328.
Hurley JH (2008). ESCRT complexes and the biogenesis of multivesicular bodies. Curr Opin Cell Biol 20, 4–11.
Jiang H, Powers TR (2008). Curvature-driven lipid sorting in a membrane tubule. Phys Rev Lett 101, 018103.
Kaetzel CS, Robinson JK, Chintalacharuvu KR, Vaerman JP, Lamm ME (1991). The polymeric immunoglobulin receptor (secretory component) mediates transport of immune complexes across epithelial cells: a local defense function for IgA. Proc Natl Acad Sci USA 88, 8796–8800.
Lippincott-Schwartz J, Yuan L, Tipper C, Amherdt M, Orci L, Klausner RD (1991). Brefeldin A's effects on endosomes, lysosomes, and the TGN suggest a general mechanism for regulating organelle structure and membrane traffic. Cell 67, 601–616.
Manders EM, Stap J, Brakenhoff GJ, van Driel R, Aten JA (1992). Dynamics of three-dimensional replication patterns during the S-phase, analysed by double labelling of DNA and confocal microscopy. J Cell Sci 103, 857–862.
Marsh EW, Leopold PL, Jones NL, Maxfield FR (1995). Oligomerized transferrin receptors are selectively retained by a lumenal sorting signal in a long-lived endocytic recycling compartment. J Cell Biol 129, 1509–1522.
Marsh M, Griffiths G, Dean GE, Mellman I, Helenius A (1986). Three-dimensional structure of endosomes in BHK-21 cells. Proc Natl Acad Sci USA 83, 2899–2903.
Massol RH, Boll W, Griffin AM, Kirchhausen T (2006). A burst of auxilin recruitment determines the onset of clathrin-coated vesicle uncoating. Proc Natl Acad Sci USA 103, 10265–10270.
Maxfield FR, McGraw TE (2004). Endocytic recycling. Nat Rev Mol Cell Biol 5, 121–132.
Mayor S, Presley JF, Maxfield FR (1993). Sorting of membrane components from endosomes and subsequent recycling to the cell surface occurs by a bulk flow process. J Cell Biol 121, 1257–1269.
Mellman I, Plutner H (1984). Internalization and degradation of macrophage Fc receptors bound to polyvalent immune complexes. J Cell Biol 98, 1170–1177.
Mellman I, Plutner H, Ukkonen P (1984). Internalization and rapid recycling of macrophage Fc receptors tagged with monovalent antireceptor antibody: possible role of a prelysosomal compartment. J Cell Biol 98, 1163–1169.
Mellman IS, Plutner H, Steinman RM, Unkeless JC, Cohn ZA (1983). Internalization and degradation of macrophage Fc receptors during receptor-mediated phagocytosis. J Cell Biol 96, 887–895.
Montoyo HP, Vaccaro C, Hafner M, Ober RJ, Mueller W, Ward ES (2009). Conditional deletion of the MHC class I-related receptor FcRn reveals the sites of IgG homeostasis in mice. Proc Natl Acad Sci USA 106, 2788–2793.
Mostov KE (1995). Regulation of protein traffic in polarized epithelial cells. Histol Histopathol 10, 423–431.
Mukherjee S, Maxfield FR (2000). Role of membrane organization and membrane domains in endocytic lipid trafficking. Traffic 1, 203–211.
Neutra MR, Ciechanover A, Owen LS, Lodish HF (1985). Intracellular transport of transferrin- and asialoorosomucoid-colloidal gold conjugates to lysosomes after receptor-mediated endocytosis. J Histochem Cytochem 33, 1134–1144.
Prabhat P, Gan Z, Chao J, Ram S, Vaccaro C, Gibbons S, Ober RJ, Ward ES (2007). Elucidation of intracellular recycling pathways leading to exocytosis of the Fc receptor, FcRn, by using multifocal plane microscopy. Proc Natl Acad Sci USA 104, 5889–5894.
Qiao SW, Kobayashi K, Johansen FE, Sollid LM, Andersen JT, Milford E, Roopenian DC, Lencer WI, Blumberg RS (2008). Dependence of antibody-mediated presentation of antigen on FcRn. Proc Natl Acad Sci USA 105, 9337–9342.
Raghavan M, Bjorkman PJ (1996). Fc receptors and their interactions with immunoglobulins. Annu Rev Cell Dev Biol 12, 181–220.
Raiborg C, Stenmark H (2009). The ESCRT machinery in endosomal sorting of ubiquitylated membrane proteins. Nature 458, 445–452.
Spiekermann GM, Finn PW, Ward ES, Dumont J, Dickinson BL, Blumberg RS, Lencer WI (2002). Receptor-mediated immunoglobulin G transport across mucosal barriers in adult life: functional expression of FcRn in the mammalian lung. J Exp Med 196, 303–310.
Szymczak AL, Workman CJ, Wang Y, Vignali KM, Dilioglou S, Vanin EF, Vignali DA (2004). Correction of multi-gene deficiency in vivo using a single "self-cleaving" 2A peptide-based retroviral vector. Nat Biotechnol 22, 589–594.
Tesar DB, Tiangco NE, Bjorkman PJ (2006). Ligand valency affects transcytosis, recycling and intracellular trafficking mediated by the neonatal Fc receptor. Traffic 7, 1127–1142.
Tzaban S, Massol RH, Yen E, Hamman W, Frank SR, Lapierre LA, Hansen SH, Goldenring JR, Blumberg RS, Lencer WI (2009). The recycling and transcytotic pathways for IgG transport by FcRn are distinct and display an inherent polarity. J Cell Biol 185, 673–684.
Ukkonen P, Lewis V, Marsh M, Helenius A, Mellman I (1986). Transport of macrophage Fc receptors and Fc receptor-bound ligands to lysosomes. J Exp Med 163, 952–971.
Utskarpen A, Massol R, van Deurs B, Lauvrak SU, Kirchhausen T, Sandvig K (2010). Shiga toxin increases formation of clathrin-coated pits through Syk kinase. PLoS One 5, e10944.